

# Quantum simulation of strong Charge-Parity violation and Peccei-Quinn mechanism

Le Bin Ho<sup>1,2,\*</sup>

<sup>1</sup>Frontier Research Institute for Interdisciplinary Sciences, Tohoku University, Sendai 980-8578, Japan

<sup>2</sup>Department of Applied Physics, Graduate School of Engineering, Tohoku University, Sendai 980-8579, Japan

(Dated: December 16, 2025)

Quantum Chromodynamics (QCD) admits a topological  $\theta$ -term that violates Charge-Parity (CP) symmetry, yet experimental indicate that  $\theta$  is nearly zero. To investigate this discrepancy in a controlled setting, we derive the Hamiltonian representation of the QCD Lagrangian and construct its (1+1)-dimensional Schwinger-model analogue. By encoding fermionic and gauge degrees of freedom into qubits using the Jordan-Wigner and quantum-link schemes, we obtain a compact Pauli Hamiltonian that retains the relevant topological vacuum structure. Ground states are prepared using a feedback-based quantum optimization protocol, enabling numerical evaluation of the vacuum energy  $E_0(\theta)$  on a few-qubit simulator. Our results show a displaced vacuum at nonzero  $\theta$  in agreement with strong-interaction expectations, and demonstrate that introducing a dynamical axion field drives the system toward  $\theta = 0$ , thereby realizing the Peccei-Quinn mechanism within a minimal quantum simulation. These results illustrate how quantum hardware can examine symmetry violation and its dynamical resolution in gauge theories.

*Introduction.* Quantum Chromodynamics (QCD) describes the fundamental interactions of quarks and gluons through the non-Abelian SU(3) gauge symmetry [1–3]. The QCD Lagrangian captures both the dynamics of quark fields and the gluon self-interactions that arise from this non-Abelian structure [3]. In addition to these standard kinetic and interaction terms, QCD also permits a topological contribution that explicitly violates Charge Parity (CP) symmetry [4, 5]. Although this term does not affect perturbative processes, it plays a central role in shaping the nonperturbative vacuum structure of the theory [6]. The most general QCD Lagrangian, including the CP-violating topological term, can be written as

$$\mathcal{L}_{\text{QCD}} = -\frac{1}{4}G_{\mu\nu}^a G^{a,\mu\nu} + \sum_f \bar{\psi}_f (i\gamma^\mu D_\mu - m_f) \psi_f + \theta \frac{g^2}{32\pi^2} G_{\mu\nu}^a \tilde{G}^{a,\mu\nu}, \quad (1)$$

where  $\psi_f$  denotes the quark field of flavor  $f$  with mass  $m_f$ ,  $g$  is the strong coupling constant, and  $\tilde{G}^{a,\mu\nu} = \frac{1}{2}\epsilon^{\mu\nu\rho\sigma}G_{\rho\sigma}^a$ . The gluon field strength tensor is defined by  $G_{\mu\nu}^a = \partial_\mu A_\nu^a - \partial_\nu A_\mu^a + g f^{abc} A_\mu^b A_\nu^c$ , where  $A_\mu^a$  are the gluon gauge fields and  $f^{abc}$  are the structure constants of the SU(3) Lie algebra. The covariant derivative acting on the quark fields takes the form  $D_\mu = \partial_\mu - igT^a A_\mu^a$ , with  $T^a$  representing the SU(3) generators satisfying the commutation relation  $[T^a, T^b] = if^{abc}T^c$ .

The first term in Eq. (1) corresponds to the kinetic and self-interaction energy of gluons, reflecting the inherent nonlinearity of non-Abelian gauge theories. The second term describes the dynamics of quarks, their Dirac mass contributions, and their interactions with gluons mediated by the color charge. The final term, proportional to the dimensionless parameter  $\theta$ , represents the strong CP-violating term. Unlike the electroweak theory, QCD allows a topological contribution that originates from

multi-sector vacuum. In the path-integral picture, the vacuum is a sum over gauge configurations labeled by a winding number  $n$  connect these sectors. The  $\theta$ -term contributes a phase  $\exp(in\theta)$  to each topological sector, which shifts the vacuum toward CP-violating configurations [4, 7, 8].

The tensor structure  $G_{\mu\nu}^a \tilde{G}^{a,\mu\nu}$  is odd under parity  $P$  and charge-parity  $CP$  transformations, therefore any nonzero  $\theta$  introduces explicit  $CP$  violation in the strong interaction. In QCD, such a violation would be expected to generate low-energy hadronic effects; for example, it induces a permanent electric dipole moment (EDM) of the neutron [9, 10]. Precision searches, however, have not observed such a signal. The current experimental bound places the neutron EDM  $|d_n| < 1.8 \times 10^{-26} e \cdot \text{cm}$  (90% C.L.) [11, 12], which implies an extraordinarily small value of  $|\theta| \lesssim 10^{-10}$ . This extreme suppression cannot be explained within the Standard Model, leading to the strong CP problem: QCD allows a large  $\theta$ , yet nature appears to choose a value extremely close to zero.

A compelling theoretical resolution is provided by the Peccei-Quinn mechanism [6, 13–15], which promotes  $\theta$  to a dynamical field associated with a spontaneously broken global  $U(1)_{\text{PQ}}$  symmetry. The resulting pseudo-Nambu-Goldstone boson, known as the axion, dynamically relaxes the effective  $\theta$  parameter to zero, thereby restoring CP symmetry in the strong interactions [6]. The axion framework not only resolves the strong CP problem but also provides a well-motivated candidate for dark matter, linking fundamental particle physics with cosmological observations [16].

Theoretical progress on the strong-CP problem is limited by the fact that the QCD vacuum is intrinsically nonperturbative and difficult to treat with conventional techniques. Conventional lattice methods struggle with real-time dynamics and  $\theta$ -dependence, while analytical techniques rely on approximations. Quantum simula-

tion provides a complementary route: instead of performing numerical sampling, one implements a controllable quantum system whose Hilbert space directly encodes the gauge theory and then measures how its vacuum responds to a  $CP$ -violating background. The (1+1)-dimensional Schwinger model retains essential features such as confinement and topological vacuum sectors, yet is sufficiently simple to be mapped to a small number of qubits and executed on near-term hardware.

In this work, we use this model to examine the microscopic origin of strong  $CP$  violation and its axionic restoration. We construct a qubit-encoded Schwinger model with a  $\theta$ -dependent electric sector, extend it to include a dynamical axion field, and prepare its vacuum using a feedback-driven quantum optimization algorithm (FALQON) [17]. By computing the ground-state energy as a function of  $\theta$ , we first identify the displaced vacuum expected for  $CP$ -violating gauge theories and then demonstrate its relaxation toward  $\theta = 0$  once the axion is activated. These results show that the Peccei-Quinn mechanism, the dynamical cancellation of  $CP$  violation, can be realized in controlled, few-qubit settings, suggesting a new avenue for probing topological gauge physics with quantum simulation.

*Lagrangian to Hamiltonian.* To express the QCD Lagrangian in a form suitable for canonical quantization, we rewrite the gluon field-strength tensor  $G_{\mu\nu}^a$  in terms of its temporal and spatial components. In analogy to electromagnetism, we define the chromoelectric and chromomagnetic fields as

$$E_i^a = G_{0i}^a, \quad B_i^a = -\frac{1}{2}\epsilon_{ijk}G_{jk}^a, \quad (2)$$

where  $i, j, k$  denote spatial indices, and  $a = 1, \dots, 8$  labels the color components of the  $SU(3)$  gauge group.

Substituting these definitions into the gauge-field part of the QCD Lagrangian

$$\mathcal{L}_{\text{gauge}} = -\frac{1}{4}G_{\mu\nu}^a G^{a,\mu\nu} + \theta \frac{g^2}{32\pi^2} G_{\mu\nu}^a \tilde{G}^{a,\mu\nu}, \quad (3)$$

and using the identity  $G_{\mu\nu}^a \tilde{G}^{a,\mu\nu} = -4\mathbf{E}^a \cdot \mathbf{B}^a$ , we obtain the Lagrangian density expressed in terms of the physical fields

$$\mathcal{L}_{\text{gauge}} = \frac{1}{2}\mathbf{E}^a \cdot \mathbf{E}^a - \frac{1}{2}\mathbf{B}^a \cdot \mathbf{B}^a + \theta \frac{g^2}{8\pi^2} \mathbf{E}^a \cdot \mathbf{B}^a. \quad (4)$$

The first two terms represent the kinetic and potential energy densities of the gluon fields, respectively, while the last term introduces the coupling between the chromoelectric and chromomagnetic fields that violates  $CP$  symmetry.

The canonical momentum conjugate to the spatial gauge field  $A_i^a$  is given by

$$\Pi_i^a = \frac{\partial \mathcal{L}_{\text{gauge}}}{\partial(\partial_0 A_i^a)} = E_i^a + \theta \frac{g^2}{8\pi^2} B_i^a, \quad (5)$$

showing that the  $\theta$ -term shifts the momentum by an amount proportional to the chromomagnetic field. This term couples the electric and magnetic sectors, thus  $\Pi_i^a$  no longer equals the electric field, and thereby modifying the canonical structure of the theory.

The Hamiltonian is then constructed via a Legendre transformation [18]

$$\begin{aligned} \mathcal{H}_{\text{gauge}} &= \Pi_i^a \partial_0 A_i^a - \mathcal{L}_{\text{gauge}} \\ &= \frac{1}{2}(\mathbf{E}^a \cdot \mathbf{E}^a + \mathbf{B}^a \cdot \mathbf{B}^a) - \theta \frac{g^2}{8\pi^2} \mathbf{E}^a \cdot \mathbf{B}^a. \end{aligned} \quad (6)$$

The first two terms represent the standard gauge-field Hamiltonian corresponding to pure QCD without  $CP$  violation. The final term, linear in the scalar product  $\mathbf{E}^a \cdot \mathbf{B}^a$ , arises directly from the  $\theta$ -term and encapsulates its  $CP$ -odd character.

Under charge conjugation  $C$  and parity  $P$  transformations, the chromoelectric and chromomagnetic fields transform as

$$\mathbf{E}^a \xrightarrow{P} -\mathbf{E}^a, \quad \mathbf{B}^a \xrightarrow{P} \mathbf{B}^a, \quad \mathbf{E}^a \xrightarrow{C} -\mathbf{E}^a, \quad \mathbf{B}^a \xrightarrow{C} -\mathbf{B}^a. \quad (7)$$

Therefore, the scalar product  $\mathbf{E}^a \cdot \mathbf{B}^a$  is odd under both  $P$  and  $CP$

$$\mathbf{E}^a \cdot \mathbf{B}^a \xrightarrow{CP} -\mathbf{E}^a \cdot \mathbf{B}^a. \quad (8)$$

Consequently, the term proportional to  $\theta \mathbf{E}^a \cdot \mathbf{B}^a$  in the Hamiltonian explicitly breaks  $CP$  symmetry. Although small in magnitude (given experimental constraints on  $\theta$ ), this term could induce observable effects such as a permanent EDM in color-neutral hadrons like the neutron [9, 10].

*Simplified (1+1)D  $U(1)$  Schwinger model.* We consider a (1+1)-dimensional Schwinger model, corresponding to one spatial and one temporal dimension [19, 20]. Despite its Abelian gauge structure, this model reproduces several nonperturbative features in QCD, including confinement of charges, a dynamically generated mass gap, and spontaneous chiral symmetry breaking in the massless limit [20–23]. It also possesses a nontrivial topological vacuum structure analogous to the  $\theta$ -vacua of QCD, allowing controlled investigations of  $CP$ -violating effects induced by a background  $\theta$ -term in (1+1) dimensions [23, 24]. Crucially, the Schwinger model admits a well-defined lattice discretization and a finite-dimensional gauge-link formulation [25], making it ideally suited for implementation on quantum computing platforms.

In (1+1) dimensions, the gauge field has only one spatial component, and the magnetic field identically vanishes. The gauge-field dynamics are therefore governed by the electric field  $E(x)$ , which serves as the canonical conjugate to the spatial gauge potential  $A_1(x)$ . The commutation relation reads  $[A_1(x), E(y)] = i\delta(x - y)$ ,

analogous to that between position and momentum in quantum mechanics. The continuum Lagrangian for a single fermion flavor coupled to this Abelian gauge field, including the topological  $\theta$ -term, can be written as

$$\mathcal{L} = \bar{\psi}(i\gamma^\mu D_\mu - m)\psi - \frac{1}{2}E^2 + \frac{\theta}{2\pi}E, \quad (9)$$

where  $D_\mu = \partial_\mu - igA_\mu$  denotes the gauge-covariant derivative and  $g$  is the coupling constant. Here, we omit the subscript  $f$  for short, such as  $m \equiv m_f$ . The first term describes the relativistic dynamics of the fermion field  $\psi$ , the second term represents the electric-field energy density, and the final term is the (1+1)D analog of the strong  $CP$  term in QCD. This  $\theta$ -term corresponds physically to a uniform background electric field, generating  $CP$ -violating effects analogous to those of the  $G_{\mu\nu}^a \tilde{G}^{a,\mu\nu}$  term in the non-Abelian case.

A Legendre transformation gives the Hamiltonian form

$$H = \int dx \left[ \psi^\dagger(x) \left( -i\gamma^1 D_1 + m\gamma^0 \right) \psi(x) + \frac{1}{2} \left( E(x) - \frac{\theta}{2\pi} \right)^2 \right],$$

where the shift  $E(x) \rightarrow E(x) - \frac{\theta}{2\pi}$  encodes the  $CP$ -odd topological term. This structure is analogous to the **E**·**B** coupling in QCD but simpler in one spatial dimension.

For quantum simulation, we adopt the Kogut–Susskind lattice discretization [26, 27], with gauge links  $U_{x,x+1} = e^{iA_{x,x+1}}$  and electric fields  $E_x$ . The discretized Hamiltonian reads

$$H = \frac{m}{2} \sum_x (-1)^x Z_x + w \sum_x (\psi_x^\dagger U_{x,x+1} \psi_{x+1} + \text{h.c.}) + \frac{g^2}{2} \sum_x \left( E_x - \frac{\theta}{2\pi} \right)^2, \quad (10)$$

where  $Z_x \equiv 1 - 2\psi_x^\dagger \psi_x$  denotes the local charge operator. The alternating sign  $(-1)^x$  stems from the staggered-fermion scheme, which suppresses fermion doubling while preserving chiral symmetry. The  $\theta$ -shift produces a uniform  $CP$ -violating background analogous to that of QCD.

To ensure gauge invariance, the Hamiltonian must satisfy Gauss's law at every lattice site. This constraint can be imposed dynamically by adding a large penalty term  $\lambda \sum_x G_x^2$ , where the generator of gauge transformations  $G_x$  is defined by

$$G_x = E_{x-1,x} - E_{x,x+1} - \psi_x^\dagger \psi_x + \eta_x. \quad (11)$$

The constant  $\eta_x$  represents a background charge determined by the staggering convention. Physical states of the theory obey  $G_x |\text{phys}\rangle = 0$ , ensuring local charge neutrality and gauge invariance.

*Two lattice sites case.* Restricting the system to its smallest nontrivial instance, i.e., two sites lattice connected by

a single link, yields the minimal Hamiltonian

$$H = \frac{m}{2}(-Z_0 + Z_1) + w(\psi_0^\dagger U_{01} \psi_1 + \text{h.c.}) + \frac{g^2}{2} \left( E - \frac{\theta}{2\pi} \right)^2 + \lambda \sum_x G_x^2. \quad (12)$$

In this representation, the first term corresponds to the staggered mass energy, the second encodes gauge-invariant fermion hopping between the two sites mediated by the link operator  $U_{01}$ , and the third term represents the electric-field energy including the  $CP$ -violating  $\theta$  shift. The final term enforces Gauss's law through an energetic constraint, restricting the evolution to the gauge-invariant subspace.

This minimal Schwinger model retains the topological and  $CP$ -violating structure of the QCD Hamiltonian while being computationally tractable on near-term quantum processors. The  $\theta$ -dependent electric-field shift plays the role of an effective  $CP$ -odd background field, allowing one to explore parity violation, vacuum degeneracy, and  $\theta$ -vacuum transitions within a low-dimensional analog of strong interactions.

To implement the model on a quantum computer, both the fermionic and gauge degrees of freedom are encoded in qubits (spin- $\frac{1}{2}$  systems). The fermionic modes are mapped to qubits using the Jordan–Wigner (JW) [28], which preserves the correct anticommutation relations through parity strings, while each gauge link is represented by a single qubit in the quantum-link formulation. The staggered fermion fields  $\psi_x$  and  $\psi_x^\dagger$  satisfy

$$\{\psi_x, \psi_y^\dagger\} = \delta_{xy}, \text{ and } \{\psi_x, \psi_y\} = 0. \quad (13)$$

In the JW representation, they are written as

$$\psi_x = \left( \prod_{y < x} Z_y \right) S_x^-, \text{ and } \psi_x^\dagger = \left( \prod_{y < x} Z_y \right) S_x^+, \quad (14)$$

where  $S_x^\pm = (X_x \pm iY_x)/2$ . The string  $\prod_{y < x} Z_y$  enforces fermionic parity between sites. Here  $X$ ,  $Y$ , and  $Z$  are Pauli matrices. The quantum-link representation of the gauge field is given by  $E = (I - Z_\ell)/2$  and  $U = (X_\ell + iY_\ell)/2$ , where  $\ell$  stands for the single-link qubit. See the End Matter section for the full derivation.

Substituting these mappings into Hamiltonian (12) yields an explicit expression in terms of Pauli matrices. The mass term, representing the energy cost of occupation on alternating sites due to the staggered fermion formulation, becomes

$$H_m = \frac{m}{2}(-Z_0 + Z_1). \quad (15)$$

The electric-field energy term, including the  $CP$ -

violating  $\theta$ -shift yields

$$\begin{aligned} H_\theta &= \frac{g^2}{2} \left( E - \frac{\theta}{2\pi} \right)^2 \\ &= \frac{g^2}{2} \left[ \left( \frac{\theta}{2\pi} \right)^2 - \frac{\theta}{2\pi} + \frac{1}{2} \right] I_l + \frac{g^2}{2} \left( \frac{\theta}{2\pi} - \frac{1}{2} \right) Z_\ell. \end{aligned} \quad (16)$$

The constant term merely shifts the global energy, while the  $Z_\ell$ -dependent term changes sign at  $\theta = \pi$ , leading to the correct  $2\pi$  periodicity.

The fermion hopping term, which describes gauge-invariant tunneling between the two sites, takes the form

$$\begin{aligned} H_{\text{hop}} &= w \left( \psi_0^\dagger U_{01} \psi_1 + \psi_1^\dagger U_{01}^\dagger \psi_0 \right) \\ &= \frac{w}{8} (X_0 X_1 X_\ell + Y_0 Y_1 X_\ell - X_0 Y_1 Y_\ell - Y_0 X_1 Y_\ell), \end{aligned} \quad (17)$$

which consists of three-body Pauli interactions coupling the two fermionic qubits with the gauge-field qubit. These terms correspond to correlated hopping processes in which a fermion moves between sites 0 and 1 while simultaneously changing the electric flux on the link, thus preserving local gauge invariance.

Finally, Gauss's law is imposed through an energy penalty term that ensures the dynamics remain confined to the gauge-invariant subspace. In Pauli form, this constraint is represented by

$$H_G = \lambda \sum_x G_x^2 = \lambda \left( \sum_{i=0,1,\ell} c_i Z_i + \sum_{i=0}^1 d_{i\ell} Z_i Z_\ell \right), \quad (18)$$

where the coefficients  $c_i, d_{i\ell} \in \{\pm \frac{1}{2}\}$  are fixed by the staggering and boundary conditions. A large  $\lambda \gg \max(m, w, g^2)$  suppresses gauge-violating excitations and confines the dynamics to the physical subspace satisfying  $G_x |\text{phys}\rangle = 0$ .

Combining all contributions, the total effective Hamiltonian for the two-site Schwinger model reaches

$$H_{\text{total}} = H_m + H_{\text{hop}} + H_\theta + H_G. \quad (19)$$

The first term encodes the fermionic mass asymmetry, the second represents correlated fermion-gauge hopping, the third incorporates the  $\theta$ -dependent  $CP$ -odd energy shift, and the last enforces gauge invariance. Despite its simplicity, this model retains the nontrivial topological and  $CP$ -violating structure of QCD and provides an ideal platform for near-term quantum simulations of gauge-theory dynamics.

*The Peccei-Quinn mechanism.* To dynamically relax the  $CP$ -violating angle, we promote  $\theta$  to a dynamical variable by introducing an axion field  $a$  with coupling scale  $f_a$ , such that

$$\theta \rightarrow \theta_{\text{eff}} = \theta + \frac{a}{f_a}. \quad (20)$$

The gauge-axion interaction term then becomes

$$H_{\theta+a} = \frac{g^2}{2} \left( E - \frac{\theta_{\text{eff}}}{2\pi} \right)^2. \quad (21)$$

The scale  $f_a$  controls how strongly the axion couples to the gauge sector, where large  $f_a$  corresponds to weak back-action and slow relaxation of  $\theta_{\text{eff}}$ , while smaller  $f_a$  enhances the axion response.

The axion degree of freedom can be represented as a periodic rotor with compact potential

$$H_a = -\kappa \cos \left( \theta + \frac{a}{f_a} \right), \quad (22)$$

which explicitly encodes the  $2\pi$  periodicity of the axion. Here,  $\kappa$  is the amplitude of the periodic axion potential, which determines how tightly the axion is pulled toward the  $CP$ -conserving minimum.

Finally, the full axion-coupled Hamiltonian is given by

$$H_{\text{total}} = H_m + H_{\text{hop}} + H_{\theta+a} + H_a + H_G. \quad (23)$$

This axion dynamics drive the effective  $CP$  phase to  $\theta_{\text{eff}} = \theta + a/f_a$ , realizing the dynamical cancellation of  $CP$  violation.

*Numerical simulation.* We compute the ground state of the two-site Schwinger-model Hamiltonian in its qubit representation using the feedback-based FALQON algorithm [17]. FALQON updates the control parameters in real time to ensure a strictly monotonic decrease of the energy expectation value, enabling ground-state preparation without any classical optimization loop. We evaluate the resulting states across different parameter regimes to examine confinement and  $CP$ -violating effects. For benchmarking and calibration, we focus on three representative configurations:

- 1. Near-continuum:**  $w = 1$ ,  $g^2 = 0.5$ ,  $m = 0.25$ , and  $\lambda = 40$ . In this limit, the system approaches the weak-coupling or near-continuum regime. Increasing the ratio  $w/g$  (i.e., decreasing  $g$ ) allows one to track how the ground-state energy and charge distribution evolve with reduced discretization effects.
- 2. Balanced benchmark:**  $w = 1$ ,  $g^2 = 1$ ,  $m = 0.25$ , and  $\lambda = 40$ . This choice provides a well-balanced regime where fermionic tunneling, gauge energy, and mass terms contribute comparably, yielding a nontrivial but numerically stable energy spectrum.
- 3. Strong gauge coupling:**  $w = 1$ ,  $g^2 = 2$ ,  $m = 0.25$ , and  $\lambda = 40$ . Increasing  $g^2$  amplifies the electric-field contribution to the energy, which reduces charge fluctuations and favors configurations with minimal local net charge.

Model	$w$	$g^2$	$m$	$\lambda$	Gauss-law	Axion
Near-continuum	1	0.5	0.25	40	$c_0 = c_1 = -\frac{1}{2}$ , $c_\ell = 0$ ,	$\kappa = g^2$ ,
Balanced benchmark	1	1	0.25	40	$d_{0\ell} = +\frac{1}{2}$ , $d_{1\ell} = -\frac{1}{2}$	$f_a = 2$
Strong gauge coupling	1	2	0.25	40		

TABLE I. **Parameter sets used in numerical simulations.** The Gauss-law and axion parameters are used for all models.

For the Gauss-law constraint, we use  $c_0 = c_1 = -\frac{1}{2}$ ,  $c_\ell = 0$ ,  $d_{0\ell} = +\frac{1}{2}$ ,  $d_{1\ell} = -\frac{1}{2}$ . For the axion sector, we set  $\kappa$  and  $f_a$  to be comparable to the gauge-field energy scale, choosing  $\kappa = g^2$ ,  $f_a = 2$ . The full parameter set is summarized in Tab. I.

Figure 1 shows the ground-state (vacuum) energy  $E_0(\theta)$  as a function of  $\theta$  for three representative parameter regimes: the near-continuum limit (blue circles), the balanced benchmark (orange triangles), and the strong gauge coupling (green triangles).

Figure 1(a) presents the ground-state energy landscape for the system without an axion field, i.e., Eq. (19). In all examined cases,  $E_0(\theta)$  reaches its minimum at a finite  $\theta = 2\pi$ . This behavior is consistent with theoretical expectations from QCD, where the vacuum energy is generally shifted away from  $\theta = 0$ , indicating a violation of  $CP$  symmetry.

Figure 1(b) shows the corresponding results after coupling the system to a dynamical axion mode, described by Eq. (23). The axion modifies the electric-field bias through the shift  $\theta \rightarrow \theta_{\text{eff}} = \theta + a/f_a$  and introduces an additional potential  $H_a$  that reshapes the vacuum structure. The resulting ground-state energy retains a  $2\pi$ -periodic profile, and the global minimum is now located at  $\theta = 0$  for all examined cases. This behavior reflects the essential Peccei-Quinn mechanism: axion back-reaction dynamically removes the  $CP$ -violating contribution to the vacuum and drives the system toward  $\theta_{\text{eff}} = 0$ . The restoration of the  $CP$ -symmetric vacuum also explains why experiments observe the physical value of  $\theta$  to lie extremely close to zero [11, 12].

These results show that even a minimal, few-qubit realization of the axion-Schwinger model captures the essential features of topological gauge interactions. As seen from the contrast between Fig. 1(a) and Fig. 1(b), the model without an axion settles at a nonzero value of  $\theta$ , consistent with the theoretical expectation from QCD that a generic  $\theta$ -term leads to  $CP$  violation. When the axion field is introduced, the system instead relaxes to  $\theta = 0$ , illustrating how the dynamical axion mechanism naturally resolves the strong  $CP$  problem.

*Extended Lattice: 4 Sites and 3 Links (7 Qubits).* Figure 2 summarizes the ground-state energy landscape of the qubit-encoded Schwinger model extended to a four-site lattice with three gauge links. The explicit Hamiltonian, including mass, gauge-mediated hopping, electric-field energy, and Gauss-law terms, is given in the End Matter section. As in Fig. 1, we evaluate the vacuum energy  $E_0(\theta)$  for three representative parameter regimes: near-continuum (blue), balanced benchmark (orange), and strong gauge coupling (green).

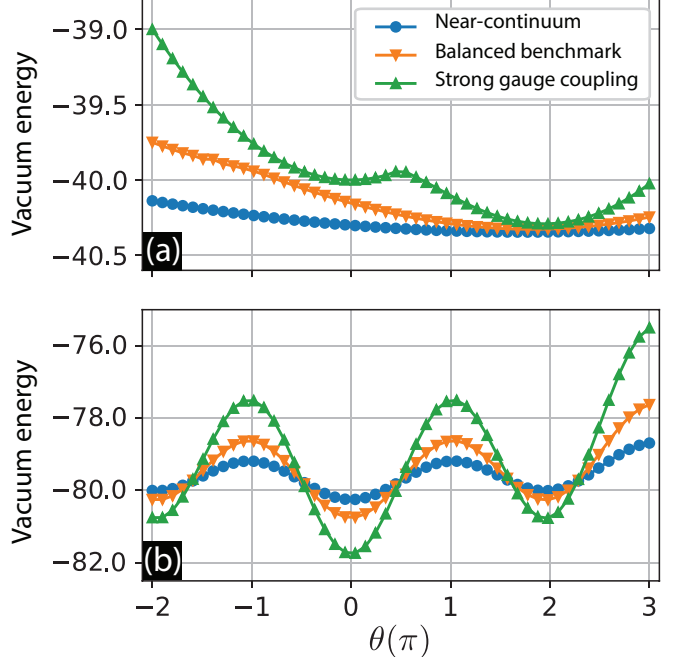


FIG. 1. **Vacuum energy of the two sites lattice Schwinger model with and without a dynamical axion.** (a) Ground (vacuum) energy  $E_0(\theta)$  of the qubit-encoded Schwinger model for three representative parameter regimes. In all cases, the minimum appears at a finite, nonzero value of  $\theta$ , consistent with the theoretical expectation that a generic  $\theta$ -term leads to  $CP$  violation in strong interactions. (b) Ground (vacuum) energy after coupling the model to a dynamical axion field. The axion back-reaction reshapes the  $\theta$ -dependent potential, producing a  $2\pi$ -periodic structure whose global minimum is pinned at  $\theta = 0$ . This shift from a displaced vacuum in (a) to a  $CP$ -symmetric vacuum in (b) shows that the axion-Schwinger construction reproduces the dynamical relaxation mechanism central to the Peccei-Quinn solution of the strong  $CP$  problem.

nian, including mass, gauge-mediated hopping, electric-field energy, and Gauss-law terms, is given in the End Matter section. As in Fig. 1, we evaluate the vacuum energy  $E_0(\theta)$  for three representative parameter regimes: near-continuum (blue), balanced benchmark (orange), and strong gauge coupling (green).

Figure 2(a) shows the case without the axion field. Similar as the two-site setup of Fig. 1(a), the enlarged lattice exhibits a displaced vacuum minimum at nonzero  $\theta = \pi$ . This behavior reflects a finite-volume effect, where in an increased number of link degrees of freedom modifies the electric-field distribution and can stabilize a non-vanishing topological angle rather than a  $CP$ -symmetric configuration.

Figure 2(b) displays the same model after coupling to a dynamical axion. As in Fig. 1(b), the axion shifts the effective vacuum angle  $\theta \rightarrow \theta_{\text{eff}}$  and introduces a periodic restoring potential. The resulting energy profile becomes explicitly  $2\pi$ -periodic, and its global minimum

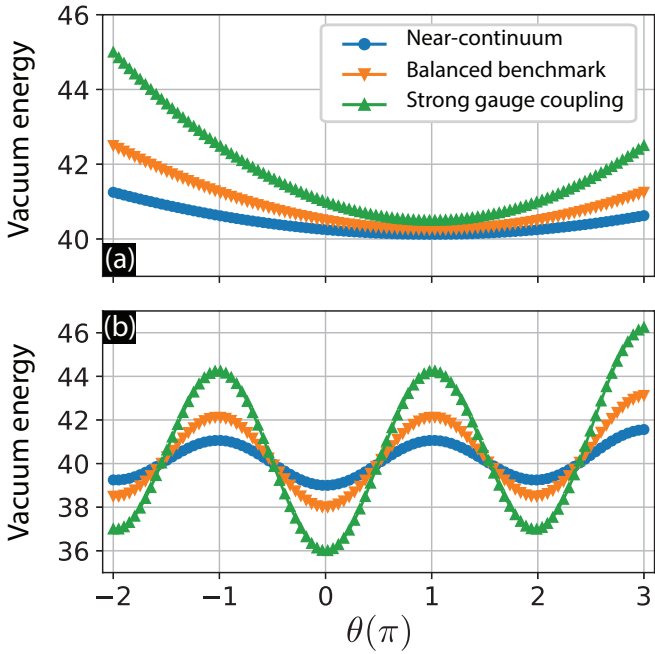


FIG. 2. **Vacuum energy of the four sites lattice Schwinger model with and without a dynamical axion.** Ground-state (vacuum) energy  $E_0(\theta)$  of the qubit-encoded Schwinger model for three representative parameter regimes, shown using the same conventions as Fig. 1 for (a) without axion field, and (b) with axion field.

is driven back to  $\theta = 0$  for all parameter regimes. This dynamical relaxation embodies the Peccei-Quinn mechanism where axion back-reaction cancels the effective  $CP$  phase and restores a  $CP$ -symmetric vacuum, even in a minimal seven-qubit realization.

**Conclusion.** Starting from the QCD Lagrangian with a  $CP$ -violating  $\theta$ -term, we derived its Hamiltonian and showed how the  $CP$ -odd contribution alters the canonical gauge structure. Reducing the theory to its  $(1+1)$ -dimensional Schwinger analogue yields a minimal model that retains key nonperturbative features, including topological vacuum structure and  $\theta$ -sensitivity. Using the Jordan-Wigner and quantum-link mappings, we express this model as an explicit Pauli Hamiltonian suitable for digital quantum simulation. We then prepared its ground state via the FALQON algorithm and evaluated the vacuum energy as a function of  $\theta$ , confirming the displaced vacuum expected from strong interactions. When a dynamical axion field is introduced, the vacuum relaxes to  $\theta = 0$ , providing a direct quantum-simulation realization of the Peccei-Quinn mechanism and a controlled framework to study  $CP$  violation and its dynamical cancellation.

**Acknowledgments.** This work is supported by the Tohoku Initiative for Fostering Global Researchers for Interdisciplinary Sciences (TI-FRIS) of MEXT's Strategic Professional Development Program for Young Researchers.

*Data availability.* No data were created or analyzed in this study.

\* Electronic address: binho@fris.tohoku.ac.jp

[1] G. 't Hooft, Quantum chromodynamics, *Annalen der Physik* **512**, 925 (2000).

[2] F. Gross, E. Klemp, S. J. Brodsky, A. J. Buras, V. D. Burkert, G. Heinrich, K. Jakobs, C. A. Meyer, K. Orginos, M. Strickland, J. Stachel, G. Zanderighi, N. Brambilla, P. Braun-Munzinger, D. Britzger, S. Capstick, T. Cohen, V. Crede, M. Constantinou, C. Davies, L. Del Debbio, A. Denig, C. DeTar, A. Deur, Y. Dokshitzer, H. G. Dosch, J. Dudek, M. Dunford, E. Epelbaum, M. A. Escobedo, H. Fritzsch, K. Fukushima, P. Gambino, D. Gillberg, S. Gottlieb, P. Grafstrom, M. Grazzini, B. Grube, A. Guskov, T. Iijima, X. Ji, F. Karsch, S. Kluth, J. B. Kogut, F. Krauss, S. Kumanou, D. Leinweber, H. Leutwyler, H.-B. Li, Y. Li, B. Malaescu, C. Mariotti, P. Maris, S. Marzani, W. Melnitchouk, J. Messchendorp, H. Meyer, R. E. Mitchell, C. Mondal, F. Nerling, S. Neubert, M. Pappagallo, S. Pastore, J. R. Peláez, A. Pickett, J. Qiu, K. Rabbertz, A. Ramos, P. Rossi, A. Rustamov, A. Schäfer, S. Scherer, M. Schindler, S. Schramm, M. Shifman, E. Shuryak, T. Sjöstrand, G. Sterman, I. W. Stewart, J. Stroth, E. Swanson, G. F. de Téramond, U. Thoma, A. Vairo, D. van Dyk, J. Vary, J. Virto, M. Vos, C. Weiss, M. Wobisch, S. L. Wu, C. Young, F. Yuan, X. Zhao, and X. Zhou, 50 years of quantum chromodynamics, *The European Physical Journal C* **83**, 1125 (2023).

[3] A. A. A. Likéné, D. N. Ongodo, P. M. Tsila, A. Atangana, and G. H. Ben-Bolie, Quantum chromodynamics lagrangian density and  $su(3)$  gauge symmetry: A fractional approach, *Modern Physics Letters A* **39**, 2450194 (2024).

[4] G. 't Hooft, Symmetry breaking through bell-jackiw anomalies, *Phys. Rev. Lett.* **37**, 8 (1976).

[5] G. 't Hooft, Computation of the quantum effects due to a four-dimensional pseudoparticle, *Phys. Rev. D* **14**, 3432 (1976).

[6] J. E. Kim and G. Carosi, Axions and the strong  $cp$  problem, *Rev. Mod. Phys.* **82**, 557 (2010).

[7] R. Jackiw and C. Rebbi, Vacuum periodicity in a yang-mills quantum theory, *Phys. Rev. Lett.* **37**, 172 (1976).

[8] H. B. Thacker and C. Xiong, Anomaly inflow and membrane dynamics in the qcd vacuum, *Phys. Rev. D* **86**, 105020 (2012).

[9] R. Crewther, P. Di Vecchia, G. Veneziano, and E. Witten, Chiral estimate of the electric dipole moment of the neutron in quantum chromodynamics, *Physics Letters B* **88**, 123 (1979).

[10] M. Pospelov and A. Ritz, Electric dipole moments as probes of new physics, *Annals of Physics* **318**, 119 (2005), special Issue.

[11] C. A. Baker, D. D. Doyle, P. Geltenbort, K. Green, M. G. D. van der Grinten, P. G. Harris, P. Iaydjiev, S. N. Ivanov, D. J. R. May, J. M. Pendlebury, J. D. Richardson, D. Shiers, and K. F. Smith, Improved experimental limit on the electric dipole moment of the neutron, *Phys. Rev. Lett.* **97**, 131801 (2006).

[12] C. Abel, S. Afach, N. J. Ayres, C. A. Baker, G. Ban, G. Bison, K. Bodek, V. Bondar, M. Burghoff, E. Chanel, Z. Chowdhuri, P.-J. Chiu, B. Clement, C. B. Crawford, M. Daum, S. Emmenegger, L. Ferraris-Bouchez, M. Fertl, P. Flaux, B. Franke, A. Fratangelo, P. Geltenbort, K. Green, W. C. Griffith, M. van der Grinten, Z. D. Grujić, P. G. Harris, L. Hayen, W. Heil, R. Henneck, V. Hélaine, N. Hild, Z. Hodge, M. Horras, P. Iaydjiev, S. N. Ivanov, M. Kasprzak, Y. Kermaidić, K. Kirch, A. Knecht, P. Knowles, H.-C. Koch, P. A. Koss, S. Komposch, A. Kozela, A. Kraft, J. Krempel, M. Kužniak, B. Lauss, T. Lefort, Y. Lemière, A. Leredde, P. Mohanmurthy, A. Mtchedlishvili, M. Musgrave, O. Naviliat-Cuncic, D. Pais, F. M. Piegza, E. Pierre, G. Piganiol, C. Plonka-Spehr, P. N. Prashanth, G. Quéméner, M. Rawlik, D. Rebreyend, I. Rienäcker, D. Ries, S. Rocca, G. Rogel, D. Rozpedzik, A. Schnabel, P. Schmidt-Wellenburg, N. Severijns, D. Shiers, R. Tavakoli Dinani, J. A. Thorne, R. Virot, J. Voigt, A. Weis, E. Wursten, G. Wyszynski, J. Zejma, J. Zenner, and G. Zsigmond, Measurement of the permanent electric dipole moment of the neutron, *Phys. Rev. Lett.* **124**, 081803 (2020).

[13] R. D. Peccei and H. R. Quinn, CP conservation in the presence of pseudoparticles, *Phys. Rev. Lett.* **38**, 1440 (1977).

[14] R. D. Peccei and H. R. Quinn, Constraints imposed by CP conservation in the presence of pseudoparticles, *Phys. Rev. D* **16**, 1791 (1977).

[15] R. D. Peccei, The strong cp problem and axions, in *Axions: Theory, Cosmology, and Experimental Searches*, edited by M. Kuster, G. Raffelt, and B. Beltrán (Springer Berlin Heidelberg, Berlin, Heidelberg, 2008) pp. 3–17.

[16] F. Chadha-Day, J. Ellis, and D. J. E. Marsh, Axion dark matter: What is it and why now?, *Science Advances* **8**, eabj3618 (2022), <https://www.science.org/doi/pdf/10.1126/sciadv.abj3618>.

[17] A. B. Magann, K. M. Rudinger, M. D. Grace, and M. Sarovar, Feedback-based quantum optimization, *Phys. Rev. Lett.* **129**, 250502 (2022).

[18] R. K. P. Zia, E. F. Redish, and S. R. McKay, Making sense of the legendre transform, *American Journal of Physics* **77**, 614 (2009).

[19] K. Aoki and T. Ichihara, (1+1)-dimensional qcd with fundamental bosons and fermions, *Phys. Rev. D* **52**, 6435 (1995).

[20] J. Schwinger, Gauge invariance and mass. ii, *Phys. Rev.* **128**, 2425 (1962).

[21] X. Luo, Spontaneous chiral-symmetry breaking of lattice qcd with massless dynamical quarks, *Science in China Series G: Physics, Mechanics and Astronomy* **50**, 6 (2007).

[22] A. Ballon-Bayona, L. A. H. Mamani, and D. M. Rodrigues, Spontaneous chiral symmetry breaking in holographic soft wall models, *Phys. Rev. D* **104**, 126029 (2021).

[23] L. Funcke, K. Jansen, and S. Kühn, Topological vacuum structure of the schwinger model with matrix product states, *Phys. Rev. D* **101**, 054507 (2020).

[24] A. V. Smilga, Vacuum fields in the schwinger model, *Phys. Rev. D* **46**, 5598 (1992).

[25] G. Calliari, M. Di Liberto, H. Pichler, and T. V. Zache, Quantum simulating continuum field theories with large-spin lattice models, *PRX Quantum* **6**, 030304 (2025).

[26] J. Kogut and L. Susskind, Hamiltonian formulation of wilson's lattice gauge theories, *Phys. Rev. D* **11**, 395 (1975).

[27] E. Zohar and M. Burrello, Formulation of lattice gauge theories for quantum simulations, *Phys. Rev. D* **91**, 054506 (2015).

[28] P. Jordan and E. Wigner, Über das paulische äquivalenzverbot, *Zeitschrift für Physik* **47**, 631 (1928).

## END MATTER

*Jordan-Wigner Transformation.* To simulate the (1+1)D lattice Schwinger model on a quantum computer, the Hamiltonian must be expressed entirely in terms of Pauli matrices acting on qubits. This requires mapping both the fermionic matter fields and the gauge link variables to spin- $\frac{1}{2}$  operators. The fermionic fields are encoded using the Jordan–Wigner (JW) transformation, while the gauge links are represented by spin operators in the quantum link model (QLM), which provides a finite-dimensional truncation of the continuous gauge degrees of freedom.

*Fermionic mapping.* The staggered fermion fields  $\psi_x$  and  $\psi_x^\dagger$  satisfy canonical anticommutation relations

$$\{\psi_x, \psi_y^\dagger\} = \delta_{xy}, \quad \{\psi_x, \psi_y\} = 0.$$

In the JW representation, these operators are mapped to Pauli operators on a chain of qubits as

$$\psi_x = \left( \prod_{y < x} Z_y \right) S_x^-, \quad \psi_x^\dagger = \left( \prod_{y < x} Z_y \right) S_x^+, \quad (24)$$

where  $S_x^\pm = (X_x \pm iY_x)/2$  are the ladder operators, and the string  $\prod_{y < x} Z_y$  encodes fermionic parity to ensure the correct anticommutation between different sites. For the minimal two-site model ( $x = 0, 1$ ), this reduces to

$$\psi_0 = S_0^-, \quad \psi_0^\dagger = S_0^+, \quad \psi_1 = Z_0 S_1^-, \quad \psi_1^\dagger = Z_0 S_1^+. \quad (25)$$

Each qubit represents one fermionic site, with the computational basis states  $|0\rangle$  and  $|1\rangle$  corresponding respectively to the unoccupied and occupied fermion configurations.

*Gauge-link mapping.* The gauge field on the link connecting sites 0 and 1 is represented by a third qubit. We denote the link qubit is  $\ell$ . In the QLM formulation, the electric field and link operators are encoded as

$$E = \frac{I - Z_\ell}{2}, \quad U_{01} = \frac{X_\ell + iY_\ell}{2}, \quad U_{01}^\dagger = \frac{X_\ell - iY_\ell}{2}. \quad (26)$$

Here,  $E$  measures the quantized electric flux on the link, while  $U_{01}$  and  $U_{01}^\dagger$  act as raising and lowering operators for the electric field, satisfying  $[E, U_{01}] = U_{01}$  and  $[E, U_{01}^\dagger] = -U_{01}^\dagger$ . The eigenvalues of  $Z_\ell$  correspond to discrete electric-field strengths  $E \in \{0, 1\}$ , providing the simplest nontrivial truncation of the gauge degree of freedom.

*Hamiltonian mapping.* Substituting these mappings into the continuum lattice Hamiltonian yields a fully qubit-based representation. The staggered-mass term, which alternates in sign to reproduce chiral symmetry in the continuum limit, becomes

$$H_m = \frac{m}{2}(-Z_0 + Z_1). \quad (27)$$

The electric-field energy, including the  $\theta$ -dependent  $CP$ -violating shift, takes the form

$$\begin{aligned} H_\theta &= \frac{g^2}{2} \left( E - \frac{\theta}{2\pi} \right)^2 \\ &= \frac{g^2}{2} \left[ \left( \frac{\theta}{2\pi} \right)^2 - \frac{\theta}{2\pi} + \frac{1}{2} \right] I_\ell + \frac{g^2}{2} \left( \frac{\theta}{2\pi} - \frac{1}{2} \right) Z_\ell. \end{aligned} \quad (28)$$

The gauge-invariant hopping term is given by

$$\begin{aligned} H_{\text{hop}} &= w(\psi_0^\dagger U_{01} \psi_1 + \psi_1^\dagger U_{01}^\dagger \psi_0) \\ &= \frac{w}{8} (X_0 X_1 X_\ell + Y_0 Y_1 X_\ell - X_0 Y_1 Y_\ell - Y_0 X_1 Y_\ell), \end{aligned} \quad (29)$$

which involves correlated three-body interactions between the two matter qubits and the gauge-link qubit, ensuring local gauge invariance.

*Gauss's law enforcement.* Local charge conservation is imposed energetically through a penalty term

$$H_G = \lambda \sum_x G_x^2 = \lambda \left( \sum_{i=0,1,\ell} c_i Z_i + \sum_{i=0}^1 d_{i\ell} Z_i Z_\ell \right), \quad (30)$$

where  $G_x$  is the Gauss-law generator and the coefficients  $c_i, d_{i\ell} \in \{\pm \frac{1}{2}\}$  are fixed by the staggering and boundary conditions.

*Final Hamiltonian.* Combining all contributions gives the complete two-site Pauli Hamiltonian,

$$H_{\text{total}} = H_m + H_{\text{hop}} + H_\theta + H_G, \quad (31)$$

where  $H_m$  encodes the fermionic mass asymmetry,  $H_{\text{hop}}$  the correlated fermion-gauge tunneling,  $H_\theta$  the  $CP$ -violating electric-field shift, and  $H_G$  enforces gauge invariance. Despite its minimal size, this model captures essential features of the Schwinger mechanism and provides a compact benchmark for near-term quantum simulations of gauge-theory dynamics.

#### Ground-state preparation via FALQON.

To obtain the ground state of the lattice Schwinger Hamiltonian, we employ the Feedback-based Algorithm for Quantum Optimization (FALQON) [17]. FALQON formulates the search for the ground state as a closed-loop quantum control problem. The system evolves under a time-dependent Hamiltonian composed of a cost

term  $H_C$  (the problem Hamiltonian) and a driver term  $H_D$  that induces state transitions:

$$H(t) = H_C + \beta(t) H_D, \quad (32)$$

where  $\beta(t)$  is a feedback control field updated at each iteration according to

$$\beta(t) = -\langle \psi(t) | i[H_D, H_C] | \psi(t) \rangle. \quad (33)$$

This choice guarantees that the expectation value of the cost energy decreases monotonically,

$$\frac{d}{dt} \langle H_C \rangle_t = -i |\langle [H_D, H_C] \rangle_t|^2 \leq 0, \quad (34)$$

ensuring convergence toward the ground state without classical optimization loops.

In discrete time, the evolution is implemented by a sequence of  $p$  alternating unitaries,

$$|\psi_{k+1}\rangle = e^{-i\Delta t \beta_k H_D} e^{-i\Delta t H_C} |\psi_k\rangle, \quad (35)$$

$$\beta_{k+1} = -\langle \psi_k | i[H_D, H_C] | \psi_k \rangle, \quad (36)$$

with time step  $\Delta t$ . In our simulations, we set  $H_C = H_{\text{total}}$  as the full Schwinger-model Hamiltonian and choose  $H_D = \sum_i X_i$  as a global mixer acting on all qubits. The FALQON feedback mechanism automatically tunes the control amplitudes  $\{\beta_k\}$  to minimize the system energy, yielding efficient and noise-robust ground-state convergence compared with traditional variational algorithms.

*Four sites and three links (7 qubits) model.* We consider a four-site open chain with three gauge links. Matter (staggered) sites are  $x = 0, 1, 2, 3$  and links are  $\ell = 4, 5, 6$  connecting  $(x, x+1)$ . In a spin- $\frac{1}{2}$  quantum link model,

$$E_\ell = \frac{I - Z_\ell}{2}, \quad U_\ell = \frac{1}{2}(X_\ell + iY_\ell). \quad (37)$$

With JW fermions, we use

$$\text{matter qubits: } q_0, q_1, q_2, q_3 \leftrightarrow x = 0, 1, 2, 3, \quad (38)$$

$$\text{link qubits: } q_4, q_5, q_6 \leftrightarrow \ell = 4, 5, 6. \quad (39)$$

The total Hamiltonian is

$$H = H_m + H_{\text{hop}} + H_\theta + H_G + \text{const.} \quad (40)$$

*Mass term.* With the standard staggered sign

$$H_m = \frac{m}{2} (-Z_{q_0} + Z_{q_1} - Z_{q_2} + Z_{q_3}). \quad (41)$$

*Gauge electric energy with  $\theta$ -term.* Using the shifted quadratic form

$$H_\theta = \frac{g^2}{2} \sum_{\ell=4}^6 \left( E_\ell - \frac{\theta}{2\pi} \right)^2, \quad E_\ell = \frac{I - Z_{q_\ell}}{2}. \quad (42)$$

*Gauge-invariant hopping.* With JW strings  $\psi_x = (\prod_{y < x} Z_{q_y}) \sigma_{q_x}^-$  and link  $U_{\ell=x+4}$  on  $(x, x+1)$ , the cancellations yield

$$\begin{aligned} H_{\text{hop}} &= w \sum_{x=0}^2 (\psi_x^\dagger U_x \psi_{x+1} + \text{h.c.}) \\ &= \frac{w}{8} \sum_{x=0}^2 \left( X_{q_x} X_{q_{x+1}} X_{q_\ell} + Y_{q_x} Y_{q_{x+1}} X_{q_\ell} \right. \\ &\quad \left. - X_{q_x} Y_{q_{x+1}} Y_{q_\ell} - Y_{q_x} X_{q_{x+1}} Y_{q_\ell} \right). \end{aligned} \quad (43)$$

*Gauss's law and penalty.* For open boundaries,

$$G_x = E_{x-1,x} - E_{x,x+1} - (n_x - \eta_x), \quad (44)$$

$$n_x = \frac{I - Z_{q_x}}{2}, \quad (45)$$

$$\eta_x = -\frac{1}{2}[1 - (-1)^x], \quad (46)$$

with  $E_{-1,0} = E_{3,4} = 0$ . We enforce gauge invariance via a large penalty and get

$$H_G = \lambda \sum_{x=0}^3 G_x^2, \quad \lambda \gg \max(m, w, g^2). \quad (47)$$